UNIVERSIDAD DE LAS AMÉRICAS PUEBLA

Escuela de Ciencias

Department of Actuarial Science, Physics and Mathematics


# Cosmology of the Early Universe with Axions

**THESIS**

José Ricardo Torres Heredia
164853

**TUTOR**

Dr. Saúl Noé Ramos Sánchez
(Instituto de Física)

San Andrés Cholula, Puebla. Fall, 2022

*Dedicated to my family.*

I wish to give thanks to my tutor, Dr. Saúl Noé Ramos Sánchez, for giving me the opportunity to do this work and for his guidance.

# Contents

# Chapter 1

# Introduction

Motivated by particle physics and suggested by several models of string theory, the axion has proven to be a fair candidate for cosmic inflation and cold dark matter. The prospect models that center themselves around the axion can be tested with multiple observations. These include observational constrains found on inflation parameters by collaborations such as Planck [1, 2, 3], as well as axion couplings probed by experimental searches [4, 5, 6, 7, 8].

In light of the strong CP (charge-parity) problem of quantum chromodynamics, the Peccei-Quinn theory was born in 1977. This managed to provide a solution by introducing a new particle called the axion [9, 10, 11, 12], associated with a scalar field. The interesting properties of such particle have given rise to multiple promising cosmological frameworks. Relevant instances of these frameworks include natural and multi-natural inflation, which attempt to reconcile the axion with the scalar field of the inflaton. These models take advantage of the periodicity of the axion potential while they seek to maintain the dynamics at energy scales that naturally arise from particle physics [13, 14]. Furthermore, on account of the weakening of the WIMP paradigm, the axion has proven to be a good candidate for dark matter [15, 16]. In fact, models have been proposed which combine inflation, reheating and dark matter as consequences of axions or axion-like particles in the so-called "ALP miracle" [17, 18]. On a different note, multiple models of string compactifications suggest the existence of this particle [19].

## Outline

In what follows, the outline of the work is presented briefly in order to serve as a guide to take the inexperienced reader through the fundamental concepts and results of the work.

### Standard Cosmology

Starting from the cosmological principle, we use Einstein's equations to derive the Friedmann equation, the acceleration equation, the continuity equation and the equation of state in its different manifestations. Once equipped with the equations to understand the dynamics of the universe, we go through a brief history of the different epochs of the universe. It is at the beginning of this history that we will then add the phenomenon of cosmic inflation from Chapter 3. Lastly, we open the discussion about the components of the universe and explore some dynamics of the universe given particular distributions of these components.

### Inflationary Cosmology

Chapter 3 gives completeness to its preceding one by introducing cosmic inflation as a useful paradigm to close previously unsolved problems of the Hot Big Bang model. Particular dynamics of the framework are introduced along with a few important parameters that will be tested against observations in order to challenge certain models of the theory. A brief mention of the more common inflationary models is made. However, the models considered in this work (explored in Chapter 5) will all be centered around the axion as the scalar field that drives inflation.

### Axions and ALPs

After a brief introduction to quantum field theory and particularly scalar fields in Chapter 4, we present the axion as the solution to the Strong CP problem of quantum chromodynamics. Later, the properties of this axion field are discussed and presented as good candidates for the inflaton and dark matter.

### Axion Models of the Early Universe

Once the axion field is introduced, several inflationary models are put forward along with the results presented for the best values of their parameters and how each model stands in the $n_s - r$ plane.

### Conclusions and Further Research

In this final section of the work, the results of the research so far are recapitulated and analyzed. This is followed by a discussion of the plans for the next stage of this research.

# Chapter 2

# Standard Cosmology

The focus of this chapter is to equip the reader with the foundational concepts and dynamic equations of cosmology that will be utilized extensively in later chapters. The following discussion is based mainly on the beginning chapters and appendices of [20] and [21], along with the second chapter of [22].

Modern cosmology rests on the assumption of the *cosmological principle*, which maintains that at large enough scales (above 100 Mpc), the universe is homogeneous and isotropic. These two properties entail, respectively, that every point in the universe has the same properties and that uniformity holds for large-scale observations at any orientation.

## 2.1 Dynamics of the Universe

In general, we want to be able to measure the separation, or difference, between two events. In special relativity, this is done using the *spacetime interval* $\Delta s^2 = -(\Delta x^0)^2 + (\Delta x^i)^2$ as the scalar product of a vector with itself. However, to ensure that we stay in an inertial reference frame, we take short enough (infinitesimal) time intervals. It is therefore convenient to instead write the spacetime interval in its differential expression[1]

$$\mathrm{d}s^2 = -(\mathrm{d}x^0)^2 + (\mathrm{d}x^i)^2 = g_{\mu\nu}\mathrm{d}x^\mu \mathrm{d}x^\nu, \tag{2.1}$$

where the $g_{\mu\nu}$ in the last equality is called the *metric*. This contains the details on how to measure distances between events, therefore encoding the geometry of our manifold. In this way, the relative sign between the time and space components that the metric introduces indicates that spacetime is not Euclidean but Minkowskian.

Once adhering to the cosmological principle, it is possible to have the geometry of i) a simple three-dimensional flat space of line element $\mathrm{d}s^2 = \mathrm{d}x$, ii) the surface of a sphere in

[1] In this differential form, the spacetime interval is also often referred to as *line element* or *line segment*.

four-dimensional Euclidian space described by $\mathrm{d}s^2 = \mathrm{d}x^2 + \mathrm{d}w^2$, and iii) a hyperspherical surface in four-dimensional Euclidean space where $\mathrm{d}s^2 = \mathrm{d}x^2 - \mathrm{d}w^2$. These cases are all included in the general line element

$$\mathrm{d}s^2 = -(\mathrm{d}t)^2 + a^2(t)\left[\frac{(\mathrm{d}r)^2}{1-kr^2} + r^2(\mathrm{d}\theta)^2 + r^2\sin^2(\theta)\mathrm{d}\phi^2\right], \tag{2.2}$$

which is written in spherical coordinates and admits a dimensionless scale factor $a(t)$ that describes the expansion of space and is conventionally normalized at actual time[2] so that $a(t_0) = 1$. Eq. (2.2) is written in natural units such that $\hbar = c = k_B = 1$. Unless otherwise stated, this work assumes natural units for simplicity. The curvature parameter $k$ can assume a value of $-1$, 0 or $+1$, corresponding respectively to a universe that is either open, flat or closed in geometry. This line segment assumes the Friedmann–Lemaître–Robertson–Walker (FLRW) metric

$$g_{\mu\nu} = \begin{pmatrix} -1 & 0 & 0 & 0 \\ 0 & \frac{a^2(t)}{1-kr^2} & 0 & 0 \\ 0 & 0 & a^2(t)r^2 & 0 \\ 0 & 0 & 0 & a^2(t)r^2\sin^2(\theta) \end{pmatrix}. \tag{2.3}$$

In order to derive the universal dynamic equations using this, we consider Einstein's field equations

$$R_{\mu\nu} - \frac{1}{2}g_{\mu\nu}R + \Lambda g_{\mu\nu} = 8\pi G T_{\mu\nu}, \tag{2.4}$$

in which $\Lambda$ is a cosmological constant, $T_{\mu\nu}$ is the energy-momentum tensor, $R_{\mu\nu}$ is the Ricci tensor[3]

$$R_{\mu\nu} = \frac{\partial\Gamma^\alpha_{\mu\nu}}{\partial x^\alpha} - \frac{\partial\Gamma^\alpha_{\alpha\mu}}{\partial x^\nu} + \Gamma^\alpha_{\alpha\beta}\Gamma^\beta_{\mu\nu} - \Gamma^\alpha_{\mu\beta}\Gamma^\beta_{\alpha\nu} \tag{2.5}$$

and $R$ is the Ricci scalar $R \equiv R^\mu{}_\mu = g^{\mu\nu}R_{\mu\nu}$, which, using the FLRW metric, becomes

$$R = 6\left(\frac{\ddot{a}}{a} + \left(\frac{\dot{a}}{a}\right)^2 + \frac{k}{a^2}\right), \tag{2.6}$$

while the non-vanishing components of the Ricci tensor become

$$R_{00} = -3\frac{\ddot{a}}{a}, \qquad R_{0i} = 0, \qquad R_{ij} = g_{ij}\left(\frac{\ddot{a}}{a} + 2\left(\frac{\dot{a}}{a}\right)^2 + 2\frac{k}{a^2}\right), \tag{2.7}$$

[2] As it is convention in cosmology, the subscript 0 in a parameter indicates this observable at its present time, labeled $t_0$.

[3] Recall that the Christoffel symbols are defined as

$$\Gamma^\mu_{\lambda\rho} \equiv \frac{1}{2}g^{\mu\nu}\left[\frac{\partial g_{\rho\nu}}{\partial x^\lambda} + \frac{\partial g_{\lambda\nu}}{\partial x^\rho} - \frac{\partial g_{\lambda\rho}}{\partial x^\nu}\right].$$

with $i$ and $j$ running over the three Cartesian coordinate directions. Let us then make the important assumption that the universe can be considered as a perfect fluid[4]. This is characterized by the equation of state

$$P = w\rho, \tag{2.8}$$

where $P(t)$ is an isotropic pressure, $\rho(t)$ is the energy density and $w$ is a dimensionless constant. Common instances of such substances include pressureless dust ($w = 0$), radiation ($w = 1/3$) and a cosmological constant $\Lambda$ ($w = -1$). The stress-energy tensor of this system takes the form

$$T_{\mu\nu} = (\rho + P)u_\mu u_\nu + Pg_{\mu\nu}, \tag{2.9}$$

with $u_\mu = (1, 0, 0, 0)$ being the four-velocity of the fluid element (considering the fluid at rest). This yields the components

$$T_{ij} = \delta_{ij}P, \qquad T_{i0} = 0, \qquad T_{00} = \rho. \tag{2.10}$$

It can be shown[5] that from the requirement that $\Delta_\mu T^{\mu\nu} = 0$, we get the condition

$$u^\mu \Delta_\mu \rho + (\rho + P)\Delta_\mu u^\mu = 0, \tag{2.11}$$

which translates into the relation

$$\dot{\rho} + 3H(\rho + P) = 0, \tag{2.12}$$

in which $H \equiv \dot{a}/a$ is the Hubble parameter. This is known as the *continuity equation*, or the *fluid equation*. Combined with eq. (2.8), it reveals that

$$\rho = \frac{\rho_0}{a^{3(w+1)}}, \tag{2.13}$$

with $\rho_0$ being an integration constant. This relation tells us how a certain energy density is diluted as the universe expands. For instance, recalling the simple examples mentioned above, we see that for dust (non-relativistic matter), $\rho_m \propto a^{-3}$, which is indeed expected for a volume increase of $a^3$. However, in the case of radiation we have a dilution in the same magnitude along with the energy loss of a power of $a^{-1}$ due to the redshift effect so that $\rho_r \propto a^{-4}$. Lastly, for the cosmological constant $\Lambda$ we simply get a constant energy density $\rho = \rho_0$.

Solving Einstein's equations using eqs. (2.6), (2.7) and (2.10), we get the temporal part of the solution as

$$H^2 = \frac{8\pi G}{3}\rho + \frac{\Lambda}{3} - \frac{k}{a^2}, \tag{2.14}$$

[4]In this sense, the inhomogeneity caused by the structures we observe in the universe is only due to our small perspective. This assumption of a perfect fluid arises from the cosmological principle.

[5]Consult [23] for more details.

known as the *Friedmann equation* and the spatial part

$$\frac{\ddot{a}}{a} = -\frac{4\pi G}{3}\big(\rho + 3P\big) + \frac{\Lambda}{3}, \tag{2.15}$$

which is often called the *acceleration equation*. With eqs. (2.8), (2.14) and (2.15) we have enough information to know the general dynamics of the universe by relating the energy density $\rho(t)$, the pressure $P(t)$ and the scale factor $a(t)$.

## 2.2 A Brief History of the Early Universe

We know from eq. (2.13) the relation between the energy density of certain components of the universe and the scale factor. Those (inverse) relations imply that tracing the universe back to a small size would lead to a very dense and hot system, this is referred to as the *primordial soup*. At this time, the typical photon energy $E_\gamma$ was much higher than the binding energy of atoms and therefore no atoms could exist yet. In fact, the number density of baryons (minus that of antibaryons) was much less than the number density of photons. The collision rate of these photons with charged particles such as electrons can be assumed to be also very high at this epoch, enough so that we may consider these particles to be in thermal equilibrium. This means that the mean-free path of photons was very small, rendering the early universe opaque. As the universe cools down (at the age of about 378,000 years old), the photon energies become unable to ionize atoms, allowing free electrons to combine with protons. This process is known as *recombination*, and it marked the beginning of the matter-dominated era. It is shortly followed by the *decoupling* process, in which the photon mean-free path grows enough to decouple light from matter, making the universe transparent. The light barrier that marked this process is known as the *last scattering surface* and its observation is one of the most important advancements in modern cosmology.

Up until this point, we have described the the Hot Big Bang (HBB) model. The other framework that completes our current understanding of the early universe is that of inflationary cosmology. This deals with an exponential rate of expansion that gives rise to the necessary conditions for the HBB. We will cover this topic in more detail in Chapter 3.

## 2.3 The Cosmic Microwave Background

Given the expansion of the universe up until our times, the radiation from the last scattering surface has weakened into the microwave range. It was accidentally discovered in 1965 by Arno Penzia and Robert Wilson from Bell Labs when they measured an unexpected constant microwave noise coming from all directions of space. Now this Cosmic Microwave

Background (CMB) radiation serves as an overwhelming confirmation of the previously assumed cosmological principle and provides insight into the dynamics and constraints of inflation. At a uniform temperature of $T_{\rm CMB} = 2.7255 \pm 0.0006$ K, it retained the black body spectrum of the early photons. However, it did not show perfect uniformity. Among the different types of anisotropies in the CMB, the most relevant to this work are the primordial anisotropies of order $\sim 10^{-5}\ T_{\rm CMB}$, to which we now briefly turn our attention. These anisotropies are created by the density perturbations of the early universe and although the Hot Big Bang cannot justify them, inflationary cosmology can offer insights about their origin. It is understood that these primordial density perturbations are the origin of the large structure formation of the universe that we observe today. The spectrum of perturbations is

$$\mathcal{P}_\zeta(k) = \mathcal{A}_s \left(\frac{k}{k_*}\right)^{n_s - 1}, \tag{2.16}$$

where $\mathcal{A}_s$ is a the constant amplitude, $k_*$ is the pivot scale[6] and $n_s$ is the scalar spectral index, which becomes

$$n_s(k) = 1 + \frac{\mathrm{d}\ln \mathcal{P}_\zeta}{\mathrm{d}\ln k}, \tag{2.17}$$

Additionally, the subscript $\zeta$ refers to the function known as curvature perturbation, although we will not explore this function in detail[7]. We also take into account the tensor perturbations from gravitational waves

$$\mathcal{P}_h(k) = \mathcal{A}_t \left(\frac{k}{k_*}\right)^{n_t}, \tag{2.18}$$

for a tensor spectral index

$$n_t(k) = \frac{\mathrm{d}\ln \mathcal{P}_h}{\mathrm{d}\ln k}. \tag{2.19}$$

Even though the spectrum of tensor perturbations has not yet been observed, CMB observations have placed constraints on these through the *tensor-to-scalar ratio*, defined as

$$r \equiv \frac{\mathcal{P}_h}{\mathcal{P}_\zeta}. \tag{2.20}$$

The constraints on several parameters mentioned here will be discussed in more detail in Chapter 5.

## 2.4 Components of the Universe

Given multiple observations (see below) which suggest a flat curvature of space, we place emphasis on this type of curvature. We define the *critical density* $\rho_c$ as that required to

[6] This is usually taken to be $k_* = 0.002$ Mpc$^{-1}$ or $k_* = 0.05$ Mpc$^{-1}$.

[7] For a more detailed discussion, see Chapter 5 of [21].

make the universe spatially flat. Using eq. (2.14) with $k = 0$ yields

$$\rho_c = \frac{3H^2}{8\pi G}. \tag{2.21}$$

We then define the *density parameter*

$$\Omega(t) \equiv \frac{\rho}{\rho_c}, \tag{2.22}$$

as the ratio of energy density in the universe and the critical energy density. The Friedmann equation can be written as

$$\Omega - 1 = \frac{k}{a^2 H^2} = \frac{k}{\dot{a}^2}. \tag{2.23}$$

From eqs. (2.22) and (2.23) we can see that

$$\begin{aligned} \rho < \rho_c \quad &\Longrightarrow \quad \Omega < 1 : k < 0 : \quad \text{Open Universe,} \\ \rho > \rho_c \quad &\Longrightarrow \quad \Omega > 1 : k > 0 : \quad \text{Closed Universe,} \\ \rho = \rho_c \quad &\Longrightarrow \quad \Omega = 1 : k = 0 : \quad \text{Flat Universe.} \end{aligned} \tag{2.24}$$

As we will see, for particular components of the universe we write $\Omega_i(t) = \rho_i/\rho_c$. Likewise, for the present state of the universe we use $\Omega_0(t) = \rho_0/\rho_c$. This is an important observable parameter often measured by collaborations such as Planck [1]. The components of the universe currently known are, as mentioned before, non-relativistic matter (including dark matter), radiation and dark energy, or the cosmological constant. The total density parameter then reads

$$\Omega_{\text{tot}} = \Omega_m + \Omega_r + \Omega_\Lambda \equiv 1, \tag{2.25}$$

and using eq. (2.13) along with eq. (2.14) for a flat universe (as we will consider from now on), we obtain

$$H^2 = \frac{8\pi G \rho_0}{3a^{3(w+1)}}, \tag{2.26}$$

from which we get

$$a(t) = \left(\frac{t}{t_0}\right)^{2/(3+3w)}, \tag{2.27}$$

which brings helpful information about the dynamics of model universes with the components taken into account.

### 2.4.1 Model Universes

Model universes are solutions to eqs. (2.14), (2.15) and (2.8) for given boundary conditions that depend on the components that the simulated universe admits. This is done to understand how the universe behaves given its contents and conventionally we consider the simplest cases[8]: single-component universes. Let us briefly explore each one of these possibilities.

#### Dust

For a universe comprised only of non-relativistic matter such as galaxies or cold dark matter, eq. (2.27) becomes

$$a(t) = \left(\frac{t}{t_0}\right)^{2/3}, \tag{2.28}$$

which shortens the age of that universe to $t_0 = 2/3H_0$. Its matter density is

$$\rho(t) = \frac{1}{6\pi G t^2}. \tag{2.29}$$

This is known as the *Einstein-de Sitter universe*.

#### Radiation

A universe filled with radiation (relativistic matter) morphs the scale factor into

$$a(t) = \left(\frac{t}{t_0}\right)^{1/2}, \tag{2.30}$$

and the age of this universe becomes $t_0 = 1/2H_0$, while its matter density scales as

$$\rho(t) = \frac{3}{32\pi G t^2}. \tag{2.31}$$

#### Cosmological Constant

For a universe containing only the vacuum energy of the cosmological constant, we have that $w = -1$ and eq. (2.27) does not apply to this. Instead, we return to eq. (2.26) to notice that $H^2$ is constant. This leads us to say that

$$a(t) \propto e^{Ht} \tag{2.32}$$

[8]Technically, there is an even simpler model: the empty universe, also known as *Milne's universe*. In this model, the universe is only affected by the curvature ($w = -1/3$) and so the energy density $\rho = 0$ and the Friedmann equation becomes simply $\dot{a}^2 = k$, while eq. (2.27) becomes $a(t) = t/t_0$.

where the Hubble constant is

$$H = \sqrt{\frac{8\pi G\rho}{3}} \tag{2.33}$$

This is known as the *de Sitter universe* or *de Sitter spacetime*. Since it only contains a cosmological constant which expands the universe, one of the main applications of this model is cosmic inflation.

## 2.5 Dark Matter

In 1933, the first evidence of dark matter arose from the work of Fritz Zwicky. In an attempt to compute the mass of the Coma cluster, Zwicky calculated a star velocity dispersion much higher than expected from the observed galaxies and their mass estimates. From this he concluded that there was a greater amount of dark matter than luminous matter in the galaxy cluster [Zwicky]. Similar conclusions were later reached by Sinclair Smith in his work estimating the mass of the Virgo cluster [history]. However, at the time neither Zwicky nor Smith argued for any explanation beyond cold stars, gases and clouds made of baryonic matter. The *Weakly Interacting Massive Particles* (WIMPs) were for some time the most promising type of particles for this. However, in the last decades, the evidence has pointed towards a non-baryonic and non-relativistic, or "cold", form of dark matter. In fact, the total matter density reported by the Planck Collaboration is $\Omega_m h^2 = 0.14240 \pm 0.00087$ [2], which corresponds to a 30% of the critical density given that $\Omega_m = 0.3111 \pm 0.0056$. From this, cold dark matter (CDM) accounts for $\Omega_{\text{CDM}} h^2 = 0.11933 \pm 0.00091$, while baryonic matter comprises only $\Omega_b h^2 = 0.02242 \pm 0.00014$. Since the fall of the WIMPs, ALPs have become promising candidates for cold dark matter.

# Chapter 3

# Cosmic Inflation

The basic idea of inflation consists in an early period of accelerated expansion of the universe due to the overwhelming potential energy of a scalar field. It was born in 1981 when Alan Guth noticed that scalar fields could get stuck in a local minimum of their potential without breaking grand unified symmetries [20]. Guth then reported that in this manner, both the horizon and flatness problems of standard cosmology could be eliminated by considering a supercooling of the universe of 28 or more orders of magnitude below the critical temperature for a phase transition [24]. However, there were flaws in the model, now referred to as "old inflation". These flaws were mainly around the phase transitions from the "false vacuum" to the "true vacuum" at the end of inflation. This would create rapidly expanding bubbles of true vacuum that would not lead to a homogeneous and isotropic universe. This came to be known as the problem of the *graceful exit*. Decades later, these drawbacks were tamed by the *new inflation* offered by Andre Linde [25] and by Andreas Albrecht and Paul J. Steinhardt [26]. This introduced the idea of a slow roll of the potential towards its minimum that modern inflationary theories are centered around.

## 3.1 Problems of the Hot Big Bang Model

Before exploring the dynamics of inflation, let us briefly motivate the theory by highlighting its usefulness around previously unsolved problems of the HBB.

### 3.1.1 The Flatness Problem

From eq. (2.23) we can trace back the history of the universe while maintaining the term on the left which we now write as $|\Omega - 1|$ in order to know the deviations from flatness at a certain point in time. Doing this we find that spacial flatness is an unstable condition and the fact that the farther back in time we go, the more precise this flatness has to

be suggests an uncomfortable fine-tuning unaccounted for by the HBB model. Indeed, at the Planck time ($t_P \sim 5 \times 10^{44}$ s), we find that $|\Omega_P - 1| \leq 2 \times 10^{-62}$ [27]. This is the predicament of the flatness problem. From eq. (2.23) we see that for a non-flat universe ($k \neq 0$) we want $\dot{a}$ to be as large as possible. As we will see shortly, inflation requires

$$\ddot{a} > 0 \quad \Longleftrightarrow \quad \frac{\mathrm{d}}{\mathrm{d}t}\left(\frac{1}{aH}\right) < 0. \tag{3.1}$$

For a $\Lambda$-dominated inflation period (this is the de Sitter spacetime we want to approximate), eq. (2.32) tells us that $a \propto e^{H_{\mathrm{ini}}t}$. The exponential period of expansion increases the scale factor by $a(t_{\mathrm{end}}) = a(t_{\mathrm{ini}})e^N$ for an e-fold number $N = H_{\mathrm{ini}}(t_{\mathrm{end}} - t_{\mathrm{ini}})$. We may consider the times it started and it ended and write

$$\frac{|\Omega(t_{\mathrm{end}}) - 1|}{|\Omega(t_{\mathrm{ini}}) - 1|} = \left(\frac{a_{\mathrm{ini}}}{a_{\mathrm{end}}}\right)^2 \equiv e^{-2N}. \tag{3.2}$$

If inflation lasts long enough, the deviations from the spatial curvature can be made arbitrarily small. The geometrical analogy for this is that a curved manifold enlarged enough would seem increasingly flat. Given observations of $\Omega_0$, it is found that $N \approx 60$ [28].

### 3.1.2 The Horizon Problem

The horizon problem is a bit more straightforward. We assume the cosmological principle in order to know the dynamics of the universe and the CMB confirms it but, why should this be the case? In fact, the CMB is precisely where this problem shows more clearly. Its relative uniformity indicates that there was thermal equilibrium between parts of the universe that, in the HBB picture, could not have been in causal contact even at the time of recombination, less than 400,000 years after the Big Bang (this is not much compared to the 13.9 billion-year history of the universe).

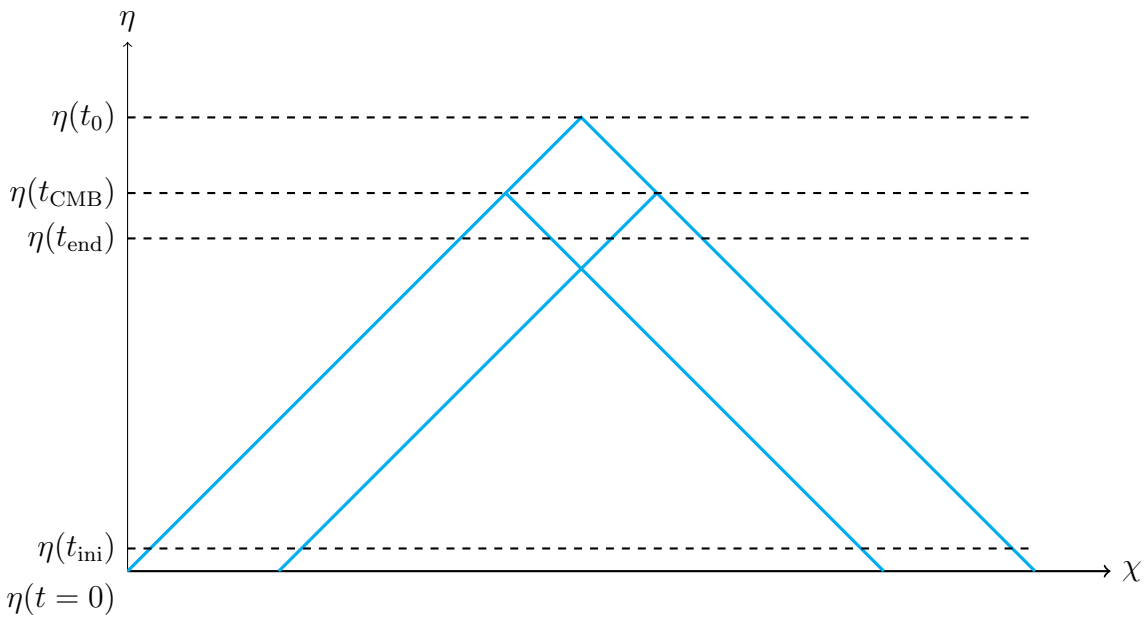


Figure 3.1: Spacetime diagram of conformal time and distance. The lightcones for two light rays observed at $t_0$ are shown to be in causal contact due to the inflationary phase, even though the opposite seems to be the case when observing until the last scattering surface.

Fortunately, the exponential expansion of the universe provides enough opportunity for thermal equilibrium in the most distant parts of the last scattering surface if inflation lasts long enough (Fig. 3.1). This constraint on the minimum time required for inflation concurs with that arising from the solution to the flatness problem [21].

While these are the main problems with the HBB model, it is worth noting that these are not the only ones. The monopole problem and the relic problem also find resolution in the inflationary paradigm [20, 21].

## 3.2 The Inflaton and its Dynamics

In order to account for the necessary properties of inflation, we introduce a homogeneous scalar field $\phi(t)$ called the *inflaton*. It is the quantum fluctuations involved in the inflationary paradigm as well as the gravitational waves of spacetime itself that give way to the perturbations explored in Section 2.3. The desired dynamics of inflation are achieved by modeling a certain potential $V(\phi)$ with a region flat enough so that the field slowly "rolls" in field space. This is so that the Hubble constant decreases slowly, yielding an exponential expansion.

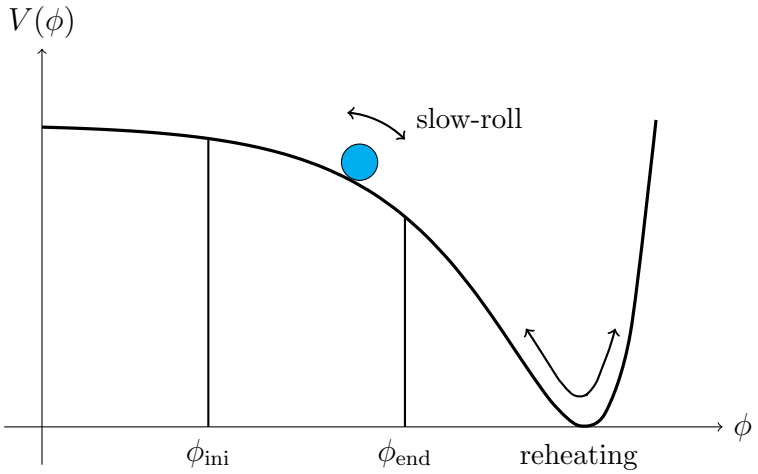


Figure 3.2: An instance of slow-roll inflation. At early times, the field portrayed in blue takes a value such that its potential $V(\phi)$ dominates over its kinetic energy. The field then rolls down the potential towards a true vacuum, eventually picking up enough kinetic energy to halt the inflationary phase.

This region in the potential encouraging a *slow-roll* of the field would be followed by a steep curve towards a minimum, in which the field would oscillate, decaying into radiation in a process called *reheating*.

The Lagrangian density for our scalar field is

$$\mathcal{L} = \frac{1}{2}\partial^\mu \partial_\mu \phi - V(\phi), \tag{3.3}$$

which leads to an equation of motion

$$\ddot{\phi} + 3H\dot{\phi} + V_{,\phi} = 0, \tag{3.4}$$

where $V_{,\phi} = \partial/\partial\phi$ and the $3H\dot{\phi}$ is visualized as a friction term which can delay the rolling of the field along its potential, ensuring slow-roll while assuring that the oscillations at the end of inflation will eventually come to rest. Assuming the field to be homogeneous we get the stress-energy tensor components

$$T_{00} = \rho_\phi = \frac{1}{2}\dot{\phi}^2 + V(\phi) \qquad \text{and} \qquad T_{ij} = P_\phi = \frac{1}{2}\dot{\phi}^2 - V(\phi)\,, \tag{3.5}$$

which turns the equation of state into

$$w_\phi = \frac{P_\phi}{\rho_\phi} = \frac{\frac{1}{2}\dot{\phi}^2 - V(\phi)}{\frac{1}{2}\dot{\phi}^2 + V(\phi)}, \tag{3.6}$$

such that in the limit $V(\phi) \gg \dot{\phi}^2$, it returns the de Sitter condition that $w \approx -1$, which implies that $\rho \approx -P$. This can also be seen by writing the acceleration equation (eq. 2.15) for the field. Furthermore, in the limit $|\ddot{\phi}| \ll |3H\dot{\phi}|$, eq. (3.4) for slow-roll (quasi-de Sitter[1]) becomes

$$3H\dot{\phi} + V_{,\phi} = 0 \qquad \Longrightarrow \qquad \dot{\phi} \simeq -\frac{V_{,\phi}}{3H}. \tag{3.7}$$

The Friedmann and acceleration equations then become

$$H^2 = \frac{8\pi G}{3}\left(\frac{\dot{\phi}^2}{2} + V(\phi)\right) \quad \text{and} \quad \frac{\ddot{a}}{a} = -\frac{8\pi G}{3}\big(\dot{\phi}^2 - V(\phi)\big). \tag{3.8}$$

When combining eqs. (2.8) and (2.15) we get

$$\frac{\ddot{a}}{a} = -\frac{4\pi G}{3}\rho(1+3w). \tag{3.9}$$

This tells us that for the period of expansion that inflation requires ($\ddot{a} > 0$) we need a pressure negative enough so that $w < -1/3$. It is precisely because of this exponential growth of the scale factor that we define the e-fold number $N$ as

$$e^N = \frac{a_{\rm end}}{a}, \qquad \text{so that} \qquad N = \ln\left(\frac{a_{\rm end}}{a}\right), \tag{3.10}$$

for some $a(t)$ during inflation. This makes sense given that as time of inflation between $a(t)$ and $a_{\rm end}(t)$ passes, $N$ tends to zero and the universe has less and less of this necessary exponential expansion to undergo. Eq. 3.10 also means that $\mathrm{d}N = -a^{-1}\mathrm{d}a = -H\mathrm{d}t$. Therefore, we can also write the e-fold number as

$$N = \int_{t_{\rm end}}^{t_{\rm ini}} H\mathrm{d}t = \int_{\phi_{\rm end}}^{\phi_{\rm ini}} \frac{H}{\dot{\phi}}\mathrm{d}\phi, \tag{3.11}$$

which corresponds to

$$N = \int_{\phi_{\rm end}}^{\phi} \frac{V}{V'}\mathrm{d}\phi = \int_{\phi}^{\phi_{\rm end}} \frac{|\mathrm{d}\phi|}{\sqrt{2\varepsilon}}. \tag{3.12}$$

It is useful to define our first *slow-roll parameter* $\varepsilon$ as

$$\varepsilon \equiv \frac{\mathrm{d}}{\mathrm{d}t}\left(\frac{1}{H}\right) = -\frac{\dot{H}}{H^2}, \tag{3.13}$$

[1]As mentioned before, de Sitter spacetime corresponds to the solution to Einstein's field equations considering only a positive cosmological constant $\Lambda$, while anti-de Sitter spacetime is the solution considering a negative cosmological constant. We use the so-called quasi-de Sitter because in order to give rise to the Hot Big Bang, the system must be in this state momentarily and eventually come to an end, as opposed to the static de Sitter spacetime.

which we can more conveniently express as

$$\varepsilon = \frac{1}{2}\left(\frac{V'}{V}\right)^2, \tag{3.14}$$

such that inflation ends at $\varepsilon(\phi_{\text{end}}) = 1$. However, at $\varepsilon = 0$ we have the de Sitter spacetime, we therefore require that $|\varepsilon| \ll 1$. As motivated in [22], in order to keep this in check we define our second slow-roll parameter

$$\eta = \frac{V''}{V}. \tag{3.15}$$

We can express the parameters introduced in Section 2.3 in terms of $\varepsilon$ and $\eta$. The spectral index is $n_s = 1 + 2\eta - 6\varepsilon$, while the tensor-to-scalar ratio is $r = 16\varepsilon$.

The drastic growth of the scale factor during inflation leads to the supercooling Guth proposed. This dissipates the content of the universe, which ends the thermal equilibrium. However, the high temperatures of the HBB model should be recovered at the end of inflation. This is accomplished if the universe goes through a process now referred to as reheating [20].

Since it was proposed, the idea of inflation has been attempted to be validated by several models. These are characterized by their scalar field potentials. One way of testing the validity of these models is through the $n_s - r$ plane subject to certain constraints provided by the observations of the CMB [1, 2]. In Chapter 5, we will introduce some inflationary models of interest and present where they currently stand against observations. As we will see, some potentials can be generalized in order to include more parameters (e.g. a phase $\theta$ inside a cosine) and do better predictions against the data. Furthermore, instead of arbitrarily choosing the parameter values, these can be optimized so that they minimize the $\chi^2$ function given by the constraints.

# Chapter 4

# Quantum Field Theory and Axions

The strong CP problem has been for some time one of the unsolved problems of particle physics. It refers to a fine-tuning problem arising from the unexpected conservation of CP symmetry in quantum chromodynamics (QCD). This problem arises from the fact that a $\theta$-*term* in the QCD Lagrangian allows for the violation of P, T and CP symmetries [29]. However, CP violation has never been observed in experiments and the $\theta$-term that theoretically allows it cannot be simply set to 0 without giving rise to further problems. The most widely accepted solution came from the Peccei-Quinn symmetry $U(1)_{\mathrm{PQ}}$ [9, 10]. This turned $\bar{\theta}$ from a constant into a dynamical variable, which relaxes to $\bar{\theta} \backsimeq 0$. Later, Frank Wilczek and Steven Weinberg both identified the breakdown of such symmetry gave rise to spin-0 massive pseudo Nambu-Goldstone bosons called *axions* [11, 12].

There exist similar postulated particles, termed axion-like particles (ALPs), which originate from Standard Model (SM) extensions[1] that introduce new symmetries, such as supersymmetry or string theory embeddings. If these symmetries are global and get spontaneously broken, NGBs or PNGBs are produced, and these may share properties of the QCD axion. This means that multiple ALPs could exist, even on top of the QCD axion.

## 4.1 Scalar and Pseudo-Scalar Fields

Recall that for the simplest classical field, we consider the Lagrangian

$$\begin{aligned} \mathcal{L} &= \frac{1}{2}\dot{\phi}^2 + \frac{1}{2}(\nabla\phi)^2 - \frac{1}{2}m^2\phi^2, \\ &= \frac{1}{2}(\partial_\mu\phi)^2 - \frac{1}{2}m^2\phi^2, \end{aligned} \tag{4.1}$$

[1] This means that ALPs are only collateral predictions of theories beyond the SM and need not fulfill any particular purpose such as solving the QCD problem. However, they can still be picked up as inflation or DM candidates.

where $m$ is interpreted as the mass of the field $\phi$. By requiring $\delta S = 0$ we get the Euler-Lagrange equations of motion

$$\partial_\mu \left( \frac{\partial \mathcal{L}}{\partial(\partial_\mu \phi_a)} \right) - \frac{\partial \mathcal{L}}{\partial \phi_a} = 0, \tag{4.2}$$

which for our Lagrangian yield

$$\partial_\mu \partial^\mu \phi + m^2 \phi = 0.$$

This is called the Klein-Gordon (KG) equation and it characterizes a free scalar field. In order to quantize, we promote the field $\phi_a(x)$ and its conjugate momentum $\pi_a(x) = \partial \mathcal{L} / \partial \dot{\phi}_a$ to operators and set the commutation relations

$$\begin{aligned} [\phi(\mathbf{x}), \phi(\mathbf{y})] = [\pi(\mathbf{x}), \pi(\mathbf{y})] = 0, \\ [\phi(\mathbf{x}), \pi(\mathbf{y})] = i\delta^{(3)}(\mathbf{x} - \mathbf{y}). \end{aligned} \tag{4.3}$$

Expanding the classical KG field in Fourier space we get

$$\phi(\mathbf{x}, t) = \int \frac{d^3 p}{(2\pi)^3} e^{i\mathbf{p}\cdot\mathbf{x}} \phi(\mathbf{p}, t), \tag{4.4}$$

and the KG equation becomes

$$\left[ \frac{\partial^2}{\partial t^2} + (|\mathbf{p}|^2 + m^2) \right] \phi(\mathbf{p}, t) = 0. \tag{4.5}$$

We recognize this as the equation for a simple harmonic oscillator which vibrates at a frequency $w_\mathbf{p} = \sqrt{|\mathbf{p}|^2 + m^2}$. We can now write

$$\begin{aligned} \phi(\mathbf{x}) &= \int \frac{d^3 p}{(2\pi)^3} \frac{1}{\sqrt{2 w_\mathbf{p}}} \left( a_\mathbf{p} e^{i\mathbf{p}\cdot\mathbf{x}} + a_\mathbf{p}^\dagger e^{-i\mathbf{p}\cdot\mathbf{x}} \right), \\ \pi(\mathbf{x}) &= \int \frac{d^3 p}{(2\pi)^3} (-i) \sqrt{\frac{w_\mathbf{p}}{2}} \left( a_\mathbf{p} e^{i\mathbf{p}\cdot\mathbf{x}} - a_\mathbf{p}^\dagger e^{-i\mathbf{p}\cdot\mathbf{x}} \right), \end{aligned} \tag{4.6}$$

where $a_\mathbf{p}$ and $a_\mathbf{p}^\dagger$ represent ladder operators that help us navigate the energy eigenvalues of a system just like those applied in the traditional harmonic oscillator quantization in introductory quantum mechanics[2]. At this point, we define the vacuum state at the point such that a lowering operator cannot apply any longer: $a_\mathbf{p}|0\rangle = 0$ for all $\mathbf{p}$. This sets the stage for particles as higher excitations in the field. We can have these particles by

[2]For more detail on this procedure, consult chapter 2 of [30].

constructing energy eigenstates from the vacuum: $|p\rangle = a^\dagger_{\mathbf{p}}|0\rangle$. If this is the case then nothing stops us from creating multiple-particle states by doing this continually so that

$$|\mathbf{p_1}, \ldots, \mathbf{p_1}\rangle = a^\dagger_{\mathbf{p_1}} \ldots a^\dagger_{\mathbf{p_n}}|0\rangle. \tag{4.7}$$

Importantly, given that the $a^\dagger$'s commute among themselves, the swapping of any two particles leaves the system the same

$$|\mathbf{p}, \mathbf{q}\rangle = |\mathbf{q}, \mathbf{p}\rangle. \tag{4.8}$$

This symmetry implies the particles are bosons. For the case of fermions, not only would we have required a different Lagrangian (such as that of the Dirac field $\mathcal{L} = \overline{\psi}(x)(i\partial\!\!\!/ - m)\psi(x)$) but we would have also needed to impose anticommutation relations $[A, B] = AB + BA = 0$ instead of those shown in eq. (4.3).

For pseudo-scalar fields, the behavior is the same as that of the scalar field except for the fact that they change sign during parity P transformations

$$(x, y, z) \quad \longrightarrow \quad (-x, -y, -z). \tag{4.9}$$

This leads to multiple consequences. For instance, the coupling of a pseudo-scalar field $\psi$ is of the form

$$\mathcal{L}_{\psi\gamma\gamma} = -\frac{g_{\psi\gamma\gamma}}{4}\psi F_{\mu\nu}\tilde{F}_{\mu\nu} = g\psi\mathbf{E}\cdot\mathbf{B}, \tag{4.10}$$

where $g_{\psi\gamma\gamma}$ is the two-photon coupling constant for the specific field, $F_{\mu\nu}$ and $\tilde{F}_{\mu\nu}$ are the electromagnetic field tensor and its dual, while $\mathbf{E}$ and $\mathbf{B}$ are the electric and magnetic fields, respectively [31, 32]. Finally, because of their definition, the parity of a boson is the same as that of its antiparticle while the parity of a fermion is opposite to that of its antiparticle.

## 4.2 Axion and ALP Dynamics

The originally proposed QCD axion introduced a complex scalar field $\psi$ through the symmetry breaking potential

$$V(\psi) = \lambda\left(|\psi|^2 - \frac{f_a^2}{2}\right)^2, \tag{4.11}$$

for some coupling $\lambda$ and a small axion decay constant $f_a$ fixed at the electroweak (EW) symmetry-breaking scale $v_{\mathrm{EW}} = 247$ GeV. This leads to big axion coupling and mass in the range $10^5 - 10^6$ eV [33]. For this reason, the original Peccei-Quinn-Weinberg-Wilczek (PQWW) model has been said to correspond to *visible axions*. However, these were soon ruled out by beam-dump [34] and other experiments and replaced by *invisible axions* with

$f_a \gg v_{\text{EW}}$ not associated to any particular energy scale [35]. With such a great $f_a$, the axion becomes light, weakly coupled and stable. The invisible axion models include the Kim-Shifman-Vainshtein-Zakharov (KSVZ) model, which introduces heavy quarks along with the $\psi$ field and differs from the Dine-Fischler-Srednicki-Zhitnitsky (DFSZ) model, which instead brings an additional Higgs field, in its lack of direct coupling to leptons [36, 33]. Just like the PQWW model, both invisible axion models spontanueously break the $U(1)_{\text{PQ}}$ symmetry by the potential from eq. 4.11 (Fig. 4.1).

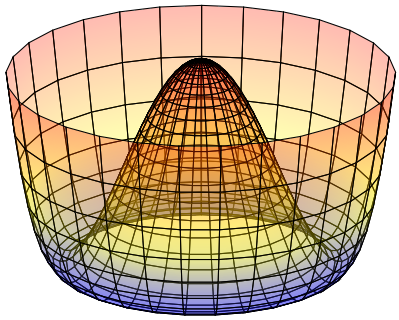

Figure 4.1: The PQWW symmetry breaking potential from eq. 4.11 in the complex plane. At the top of the hill the system maintains a rotational ($U(1)_{\text{PQ}}$) symmetry, which is spontaneously broken when the system falls to a vacuum state. From the angular degree of freedom, the VEV can be written as $\langle\psi\rangle = f_a/\sqrt{2}e^{i\phi/f_a}$ and the axion field $\phi = \psi f_a$ corresponds to the NG boson arising from fluctuations between vacuum states in this angular direction at the potential minima.

Constraints were later found from astrophysics stemming from the fact that these new weakly interacting axions provided a cooling mechanism for stars. Being produced in hot plasmas such as the interiors of stars, they will not interact much and escape, contributing to the energy loss of the star. The axion mass $m_a$ should therefore be bounded so as to not significantly shorten stellar lifetimes. This mass can be obtained through couplings to other particles. Indeed, the axion mass is related to the pion mass by $m_a f_a \approx m_\pi f_\pi$ [37], this leads to

$$m_a = \frac{m_\pi f_\pi}{f_a}\frac{\sqrt{m_u m_d}}{m_u + m_d} \simeq 6 \times 10^{-6}\ \text{eV}\left(\frac{10^{12}\ \text{GeV}}{f_a}\right), \tag{4.12}$$

where $m_u$ and $m_d$ are the up and down quark masses, respectively [12]. Similarly, the axion coupling to photons is given by

$$g_{a\gamma} = \frac{\alpha}{2\pi f_a}\left(C_{a\gamma} - \frac{2}{3}\frac{m_u + 4m_d}{m_u + m_d}\right) \simeq 10^{-13}\ \text{GeV}^{-1}\left(\frac{10^{10}\ \text{GeV}}{f_a}\right), \tag{4.13}$$

where $\alpha$ is the fine-structure constant and $C_{a\gamma}$ is a model-dependent parameter due to the electromagnetic anomaly [16]. The fact that $m_a, g_{a\gamma} \propto f_a^{-1}$, shows that the greater the decay constant $f_a$, the lighter and weakly coupled the axion. From ther latest observations we have that $f_a \sim 10^9 - 10^{12}$ GeV [33], which implies that $m_a \sim 10^{-6} - 10^{-3}$ eV and $g_{a\gamma} \sim 10^{-15} - 10^{-12}$ GeV$^{-1}$.

ALPs are expected to have the same two-photon couplings as the QCD axion although, in general, their masses and couplings are free parameters (independent from $f_a$) and can therefore be much less that that of the QCD axions [36]. This is one of the main differences between the QCD axion and ALPs. Furthermore, QCD axion and ALP candidates seem to naturally arise from string compactifications. In particular, conveniently small couplings arise from the large string energy scale involved [16]. However, these models do not necessarily predict the existence of such particles, given that they can be suppressed by other mechanisms [31].

## 4.3 Experimental Searches for Axions

### Axion Helioscope

Helioscopes directly search for axions and ALPs from the sun by pointing a strong magnet in their direction, allowing for a conversion into photons through the Primakoff effect. The CERN Axion Solar Telescope (CAST) was reported to have an upper limit of ALP-photon couplings of $g_{a\gamma} \lesssim 3.3 \times 10^{-10}$ GeV$^{-1}$ at 95% CL [38]. The next-generation experiment, the International Axion Observatory (IAXO), is being built with a projected sensitivity to detect ALP-photon couplings as small as $g_{a\gamma} \sim 2 \times 10^{-12}$GeV$^{-1}$ and ALP-electron couplings as $g_{ae} \sim 10^{-13}$ GeV$^{-1}$ for masses of 1 meV $\leq m_a \leq$ 1eV [4].

### Axion Haloscope

Haloscopes search for galactic halo made of axion or ALP dark matter. This is usually done with magnetic fields inside resonant cavities. The Axion Dark Matter eXperiment (ADMX) currently probes for axions in the $2.66 - 3.1$ $\mu$eV mass range [39]. Additionally, a search was performed using the 18 T High-Temperature Superconducting (HTS) axion haloscope in the $4.7789 - 4.8094$ GHz range. However, no significant result has been found yet [40]. The proposed Cosmic Axion Spin Precession Experiment (CASPEr) claimed a future sensitivity of $m_a \lesssim 10^{-9}$ eV for QCD axion masses corresponding to axion decay constants $f_a \gtrsim 10^{16}$ GeV [7].

### Light-Shining-Through-Wall Searches

Light-Shining-Through-Wall (LSW) experiments seek both producing and detecting axions and ALPs in the laboratory. This is attempted by sending photons through a strong

magnetic field that converts them to axions or ALPs and into a wall through which these can travel freely, only to be reconverted to photons with a second magnet at the other end, where they can be detected. The best attempt at this came from the Any Light Particle Search (ALPS) I at DESY in Germany, which achieved the best accuracy of its time, while the subsequent ALPS II experiment is currently being built with the intention of achieving 95% confidence-level detection of ALP-photon coupling constants as low as $g_{a\gamma} = 2 \times 10^{-11}$ GeV$^{-1}$ for masses below 0.1 meV [8].

# Chapter 5

# Axion Models of the Early Universe

The values assumed in this section are $n_s = 0.9665 \pm 0.0038$, $n_s' = -0.0045 \pm 0.067$ [1], and $r_{0.05} = 0.014^{+0.010}_{-0.011}$ ($r_{0.05} < 0.036$ at 95% CL) [3]. For every inflation model described below, a `Python` code was implemented to numerically compute values for $n_s$ and $r$. This was done by applying different `scipy`-integrated methods to find the roots to[1]

$$F(\phi_{\rm end}) = \epsilon(\phi_{\rm end}) - 1, \tag{5.1}$$

to obtain $\phi_{\rm end}$ and use this value to compute an array of values for $\phi_{\rm ini}$ via a trapezoidal integration. These values are then used to obtain $n_s(\phi)$ and $r(\phi)$. To this code the optimized non-linear minimization interface `lmfit` [41] was applied to find the best parameter values that minimize the $\chi^2$ function. Furthermore, the parameter space and distributions for each model were explored using the Markov Chain Monte Carlo (MCMC) sampler `emcee` included in the interface. For the sake of simplicity, from now on (unless otherwise stated) we use geometric units such that $m_P = G = 1$.

## 5.1 Models of Axion Inflation

It is worth noting that there are other models in which he axion plays the role of inflation such as hybrid inflation and the string-motivated racetract inflation and $N$-flation.

### 5.1.1 Natural Inflation

In 1990, Katherine Freese et al. introduced the case of a pseudo Nambu-Goldstone boson with a potential of the form

$$V(\phi) = \Lambda^4 \left[1 - \cos\left(\frac{\phi}{f}\right)\right], \tag{5.2}$$

[1] This is due to the condition $\epsilon(\phi_{\rm end}) = 1$.

arising from spontaneous symmetry breaking that could give rise to inflation in the scale of an axion decay constant $f \approx m_{\rm P}$ and $\Lambda \approx m_{\rm GUT} \approx 10^{15}$ GeV [13]. This is why it is the most common type of small-field model[2]. Due to the motivations from naturalness of the original idea [43], this model has come to be known as *natural inflation*. The potential of the model is shown in Fig. 5.1 and its slow-roll parameters take the form

$$\varepsilon = \frac{1}{2f^2}\frac{1+\cos\left(\frac{\phi}{f}\right)}{1-\cos\left(\frac{\phi}{f}\right)} \quad \text{and} \quad \eta = \frac{1}{f^2}\frac{\cos\left(\frac{\phi}{f}\right)}{1-\cos\left(\frac{\phi}{f}\right)}. \tag{5.3}$$

From this we find that

$$n_s = 1 - \frac{1}{f^2} - 4\varepsilon, \quad \text{and} \quad r = 16\varepsilon = 4\left(1 - n_s - \frac{1}{f^2}\right). \tag{5.4}$$

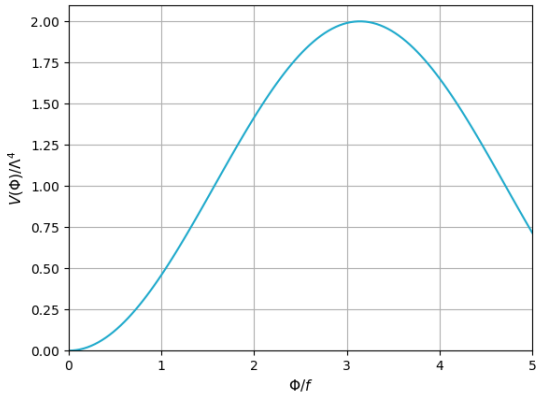


Figure 5.1: The natural inflation potential satisfies the slow-roll condition at large scales ($f = pm_P > m_P$).

[2]As the name suggests, in small-field models, the field moves over small distances $\Delta\phi < m_P$ and often emerge from spontaneous symmetry breaking [42].

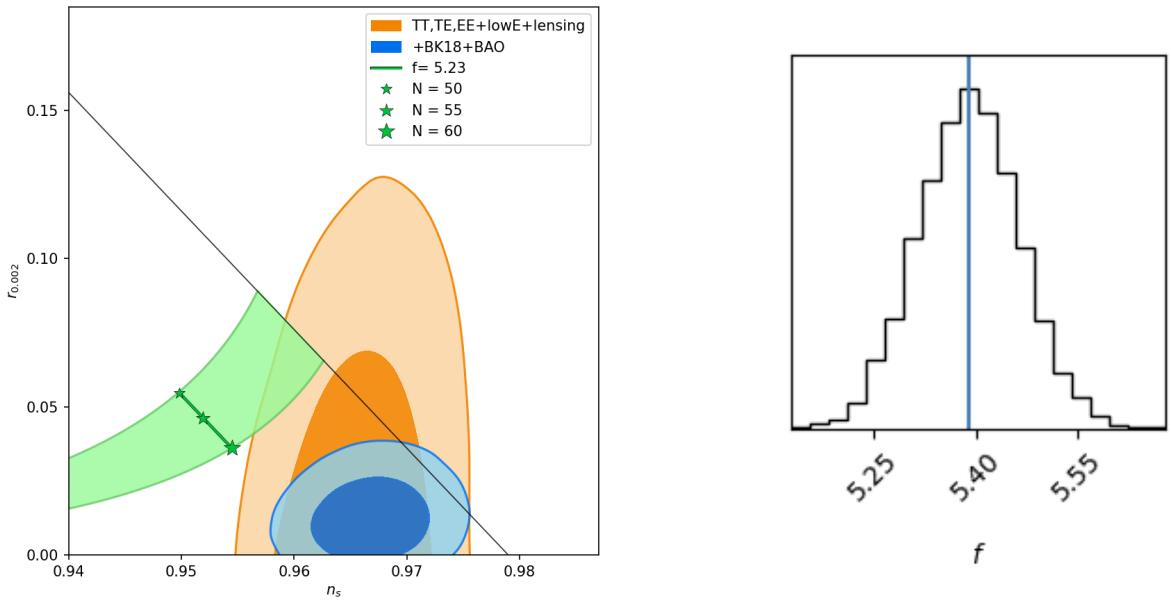


(a) $n_s - r$ plane prediction

(b) Parameter distribution

Figure 5.2: (a) The standard natural inflation prediction (with $A = 1$ and $\theta = 0$). The shaded region comprises the range of $N$ for a given decay constant $f$ until the upper bound $f < 6.89$ which is found analytically from eq (5.4) and is marked by the black line. (b) We obtain a median value of $f = 5.3891$ along with the standard deviations $-2\sigma = -0.1436$, $-1\sigma = -0.0746$, $1\sigma = 0.0746$ and $2\sigma = 0.1429$.

For the case of eq. (5.2) we obtain the parameter value $f = 5.38$ using the least-squares method from `lmfit`. The corresponding prediction is shown in Fig. (5.2a) as the best value among the possible values from $N \in [50, 60]$.

### 5.1.2 Axion Monodromy

From certain string compactifications, researchers have suggested a way to obtain large-field inflation through the monodromy induced on a brane living in a Nil manifold [44, 45]. We refer to this as *axion monodromy inflation*. Its general potential (Fig. 5.3) can be written as

$$V(\phi) = \Lambda^4 \left[ \left( \frac{\phi}{\mu} \right)^p + b \cos \left( \frac{\phi}{f} + \theta \right) \right]. \tag{5.5}$$

In this case, eq. (5.1), takes the form

$$F(\phi) = \frac{\left[ pf \left( \frac{\phi}{\mu} \right)^p - b\phi \sin \left( \theta + \frac{\phi}{f} \right) \right]^2}{2f^2\phi^2 \left[ \left( \frac{\phi}{\mu} \right) + b \cos \left( \theta + \frac{\phi}{f} \right) \right]^2} - 1. \tag{5.6}$$

The prediction for this model is shown in Fig. 5.4.

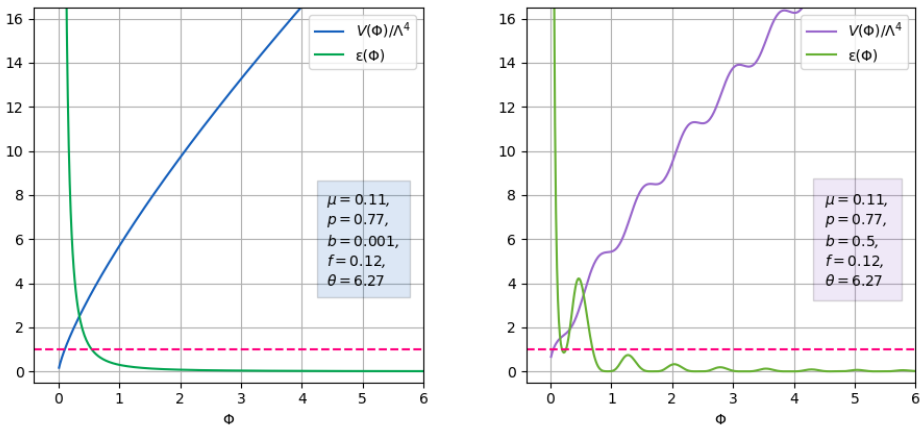


Figure 5.3: Arbitrary parameter values were chosen to illustrate the oscillatory behaviour of the potential against a continuous slow-roll for a smaller amplitude $b$.

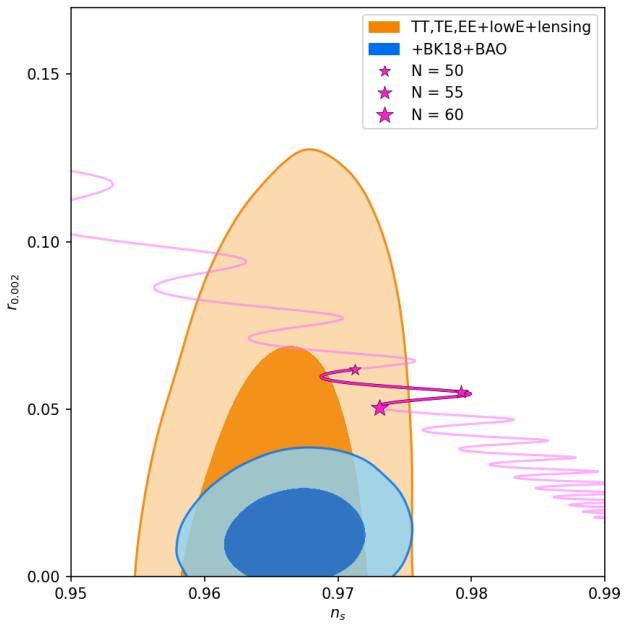


Figure 5.4: Prediction for axion monodromy by a least-squares minimization with the Levenberg-Marquardt method 17.4525. The parameter values obtained were $\mu = 0.105$, $p = 0.772$, $b = 0.001$, $f = 0.119$ and $\theta = 6.266$. A fainter curve marks the prediction for a much more extensive range of $N$, given such parameter values.

### 5.1.3 The ALP Miracle

In analogy to the WIMP miracle[3], the ALP miracle refers to a way of unifying inflation and dark matter through a single axion-like particle. It was found that for an axion-like field in a hilltop potential the same effective mass is achieved both at the beginning and at the end of inflation. Thorough a coupling to photons, most ALPs evaporate and the remnants become dark matter. Given CMB and matter power spectrum observations, both the mass and axion-photon coupling share a region inside the observation range of the next generation axion helioscope, IAXO, and other future laser experiments for the detection of axions. This coincidence is referred to as the ALP miracle and it was reached through an axion hilltop inflaton potential. Parting from natural inflation, let us now consider a single-field inflaton with two sinusoidal potentials which allow it to realize both large-field and small-field inflation [14]. This model, now called *multi-natural inflation*, has a potential

$$V(\phi) = -\Lambda_1^4 \cos\left(\frac{\phi}{f_1}\right) - \Lambda_2^4 \cos\left(\frac{\phi}{f_2} + \theta\right) + C, \tag{5.7}$$

with two decay constants $f_1$ and $f_2$ and a regular constant $C$ to keep the potential minimum at zero[4]. From this, it is possible to manipulate the variables such that we get a single axion decay constant and newly defined define. This so-called minimal axion hilltop potential is of the form

$$V(\phi) = \Lambda^4 \left[ \cos\left(\frac{\phi}{f} + \theta\right) - \frac{\kappa}{n^2} \cos\left(\frac{n\phi}{f}\right) \right] + C, \tag{5.8}$$

where we now have an integer $n > 1$ and a numerical coefficient $\kappa$ [17]. This is shown in Fig. 5.5. The parity of $n$ is responsible for the shape of the potential and the relations between the ALP mass $m_\phi$ and decay constant $f_\phi$. For a odd integer $n$. This corresponds to a massless inflaton at the maximum ($\phi = 0$) and minimum ($\phi = \pi f$).

[3]The WIMP miracle refers to the coincidental prediction from supersymmetric extensions of the standard model of a particle with dark matter properties. However, experiments failed to provide evidence for both WIMPs and supersymmetry.

[4]It is common practice to

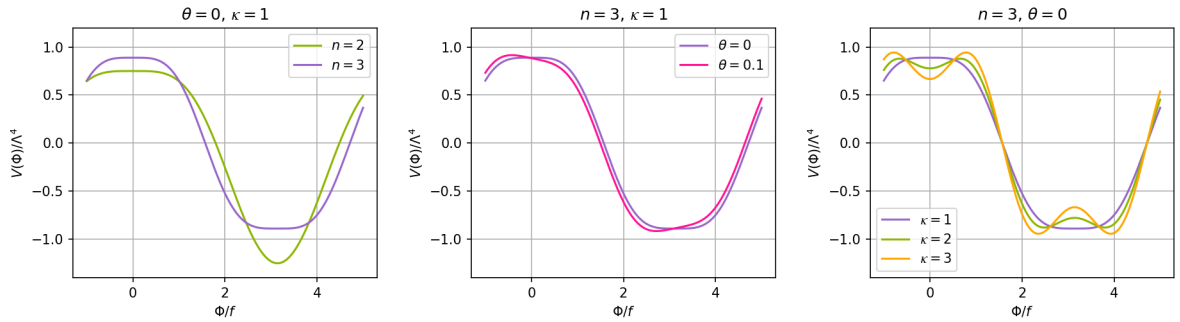


Figure 5.5: The minimal axion hilltop inflation potential for $n = 2, 3, 4$ and 5, with the phase $\theta = 0$ and rest of the parameters set to 1. For the values $\kappa = 1$ and $\theta \neq 0$, the model reduces to quartic hilltop inflation.

In order to render a more precise root-finding of eq. 5.1, we restrict the range of the `ridder` method to that spanned by $\varepsilon(\phi)$ while it satisfies the condition that $\varepsilon < 1$ (Fig. 5.6).

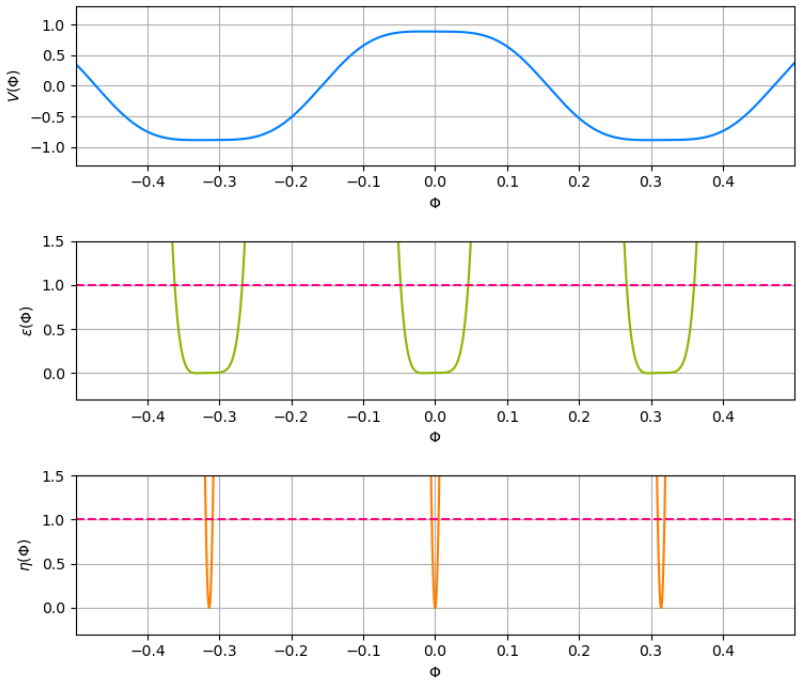


Figure 5.6: The model slow-roll parameters assuming $n = 3$, $\kappa = 1$, $f = 0.1$, $\theta = 0.007$ and $C = 0$.

Successful reheating after inflation is possible through the ALP coupling to photons.

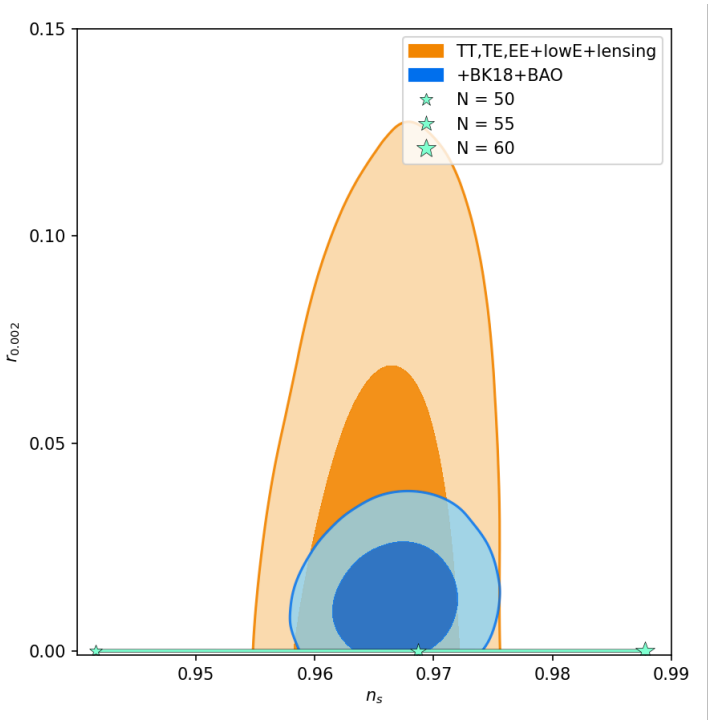


Figure 5.7: $n_s - r$ plane prediction for the axionic hilltop inflation.

The best parameters found were $n = 3$, $\kappa = 1$, $f = 2.983$, $\theta = 0.005$ and $C = -0.0184$. These provide a decent prediction inside the $1\sigma$ region. The disadvantage of this if that the model need to compromise with a high (trans-planckian) value of $f$. Previous authors have managed to get this parameter to lower values [18]. However, as the authors express, the e-fold number becomes compromised and set to close to $N = 30$, which is much smaller than what is needed to solve the horizon and flatness problems. On top of this, $\varepsilon$ was neglected in the running of the spectral index, which might imply lower accuracy.

# Chapter 6

# Conclusions

In this work, some models of inflation with axions or ALPs have been explored along with their predictions. The models considered were natural inflation, axion monodromy and inflation from axionic hilltop potential. There are multiple other models of inflation involving axions such as assisted inflation, a simple example of which is N-flation, pseudo-natural inflation involving a coupling constant [46], racetrack inflation [47] and others. Although this would make for interesting analysis, these were not included in this work. The standard form of the natural inflation potential is inconsistent with observations at greater than 95% confidence. However, attempts at refining natural inflation through protracted reheating have been made and offer additional possibilities such as consistency with the 95% confidence region, while bringing it into the 65% confidence region, although possible through a tweaking of energy scales, has proven to be a less promising ambition.

A similar inconsistency was found for inflation from an axion monodromy, although in this case, it is at least possible to bring the prediction to within a $3\sigma$ region.

Finally, while the premise of unified inflation and dark matter with a minimal axion hilltop model appears very promising, it proves to be inconsistent with the constraints on the e-fold number $N$ conventionally accepted from the resolutions to the flatness and horizon problems. Nevertheless, the model itself still poses an interesting possibility. For instance, previous works have attempted to make it work in a framework for unified inflation and dynamical dark matter [48]. It was shown to be possible to explore an infinite Kaluza-Klein tower originated from a axion-like field and the compactification of an extra dimension, and have this particle adopt the role of the inflaton in the early universe and subsequently play the part of dark matter. An important point to specify is that corner plots exploring the distributions using Markov Chain Monte Carlo analysis were made using the `emcee` package from `lmfit`. Unfortunately, by the end of this research the updating of these plots proved complicated and for technical problems it was not possible to include them in the analysis. However, it remains a great method of exploration of the distributions of parameters for future work.

On this note of future research, a more complete exploration of inflationary models

could be made by incorporating additional relevant functions (such as $\mathcal{A}_{\mathcal{S}}$, $\mathrm{d}^2 n_s/\mathrm{dln}k^2$, $n_t$ and HFFs) in the $\chi^2$ minimization, as well as considering more general expressions of the potentials along with the $\Lambda^4 = V_0$ term in the parameter variations. Mainly, however, these models remain dependent on the observations to be made by axion search experiments and it is expected that these will further constraint the values for axion masses and couplings.

# Bibliography


[1] Planck, Y. Akrami et al., *Planck 2018 results. x. constraints on inflation*, Astron. Astrophys. **641** (2020), A10, arXiv:1807.06211 [astro-ph.CO].

[2] N. Aghanim et al., *Planck 2018 results. vi. cosmological parameters*, Astron. Astrophys. **641** (2020), A6, https://doi.org/10.1051%2F0004-6361%2F201833910.

[3] P. A. et al., *Improved constraints on primordial gravitational waves using planck, wmap, and bicep/keck observations through the 2018 observing season*, Physical Review Letters **127** (2021), no. 15, https://doi.org/10.1103%2Fphysrevlett.127.151301.

[4] E. Armengaud et al., *Physics potential of the international axion observatory (iaxo)*, Journal of Cosmology and Astroparticle Physics **2019** (2019), no. 06, 047, https://dx.doi.org/10.1088/1475-7516/2019/06/047.

[5] J. K. Vogel et al., *The next generation of axion helioscopes: The international axion observatory (iaxo)*, Phys. Procedia **61** (2015), 193–200. 8 p, https://cds.cern.ch/record/2066987.

[6] B. Lakić, *International axion observatory (iaxo) status and prospects*, Journal of Physics: Conference Series **1342** (2020), no. 1.

[7] D. Budker, P. W. Graham, M. Ledbetter, S. Rajendran, and A. O. Sushkov, *Proposal for a cosmic axion spin precession experiment (casper)*, Physical Review X **4** (2014), no. 2, https://doi.org/10.1103%2Fphysrevx.4.021030.

[8] M. D. Ortiz, J. Gleason, H. Grote, A. Hallal, M. T. Hartman, H. Hollis, K. S. Isleif, A. James, K. Karan, T. Kozlowski, A. Lindner, G. Messineo, G. Mueller, J. H. Poeld, R. C. G. Smith, A. D. Spector, D. B. Tanner, L. W. Wei, and B. Willke, *Design of the alps ii optical system*, 2021.

[9] R. D. Peccei and H. R. Quinn, CP *conservation in the presence of pseudoparticles*, Phys. Rev. Lett. **38** (1977), 1440–1443.

[10] R. D. Peccei and H. R. Quinn, *Constraints imposed by* CP *conservation in the presence of pseudoparticles*, Phys. Rev. D **16** (1977), 1791–1797.

[11] F. Wilczek, *Problem of strong p and t invariance in the presence of instantons*, Phys. Rev. Lett. **40** (1978), 279–282.

[12] S. Weinberg, *A new light boson?*, Phys. Rev. Lett. **40** (1978), 223–226.

[13] K. Freese, J. A. Frieman, and A. V. Olinto, *Natural inflation with pseudo - nambu-goldstone bosons*, Phys. Rev. Lett. **65** (1990), 3233–3236.

[14] M. Czerny and F. Takahashi, *Multi-natural inflation*, Physics Letters B **733** (2014), 241–246, https://doi.org/10.1016%2Fj.physletb.2014.04.039.

[15] J. E. Kim and G. Carosi, *Axions and the strong cp problem*, Rev. Mod. Phys. **82** (2010), 557–601.

[16] A. Ringwald, *Exploring the role of axions and other wisps in the dark universe*, 2012.

[17] R. Daido, F. Takahashi, and W. Yin, *The alp miracle: unified inflaton and dark matter*, Journal of Cosmology and Astroparticle Physics **2017** (2017), no. 05, 044–044.

[18] R. Daido, F. Takahashi, and W. Yin, *The alp miracle revisited*, Journal of High Energy Physics **2018** (2018), no. 2.

[19] P. Svrcek and E. Witten, *Axions in string theory*, Journal of High Energy Physics **2006** (2006), no. 06, 051–051.

[20] S. Weinberg, *Cosmology*, Oxford University Press, 2008.

[21] K. Dimopoulos, *Introduction to cosmic inflation and dark energy*, CRC Press, 2020, https://doi.org/10.1201/9781351174862.

[22] O. Piattella, *Lecture notes in cosmology*, Springer International Publishing, 2018, https://doi.org/10.1007%2F978-3-319-95570-4.

[23] B. Schutz, *A first course in general relativity*, 2 ed., Cambridge University Press, 2009.

[24] A. H. Guth, *Inflationary universe: A possible solution to the horizon and flatness problems*, Phys. Rev. D **23** (1981), 347–356, https://link.aps.org/doi/10.1103/PhysRevD.23.347.

[25] A. D. Linde, *A new inflationary universe scenario: A possible solution of the horizon, flatness, homogeneity, isotropy and primordial monopole problems*, Phys. Lett. B **108** (1982), 389–393.

[26] A. Albrecht and P. J. Steinhardt, *Cosmology for grand unified theories with radiatively induced symmetry breaking*, Phys. Rev. Lett. **48** (1982), 1220–1223, https://link.aps.org/doi/10.1103/PhysRevLett.48.1220.

[27] B. Ryden, *Introduction to cosmology*, Cambridge University Press, 1970.

[28] J. A. V. Gonzalez, L. E. Padilla, and T. Matos, *Inflationary cosmology: from theory to observations*, Revista Mexicana de Física E **17** (2020), no. 1 Jan-Jun, 73–91, https://doi.org/10.31349%2Frevmexfise.17.73.

[29] I. I. Bigi and A. I. Sanda, *Cp violation*, 2 ed., Cambridge University Press, 2009.

[30] M. E. Peskin and D. V. Schroeder, *An Introduction to Quantum Field Theory*, Westview Press, 1995, Reading, USA: Addison-Wesley (1995) 842 p.

[31] J. Jaeckel and A. Ringwald, *The low-energy frontier of particle physics*, Annual Review of Nuclear and Particle Science **60** (2010), no. 1, 405–437, https://doi.org/10.1146/annurev.nucl.012809.104433, https://doi.org/10.1146/annurev.nucl.012809.104433.

[32] A. J. Powell, *The cosmology and astrophysics of axion-like particles*, 2016.

[33] A. Ayad, *Phenomenological aspects of axion-like particles in cosmology and astrophysics*, 2022.

[34] J. E. Kim, *Light Pseudoscalars, Particle Physics and Cosmology*, Phys. Rept. **150** (1987), 1–177.

[35] D. J. Marsh, *Axion cosmology*, Physics Reports **643** (2016), 1–79, https://doi.org/10.1016%2Fj.physrep.2016.06.005.

[36] D. J. Marsh, *Axion cosmology*, Physics Reports **643** (2016), 1–79, https://doi.org/10.1016%2Fj.physrep.2016.06.005.

[37] K. Olive, *Review of particle physics*, Chinese Physics C **38** (2014), no. 9, 090001, https://dx.doi.org/10.1088/1674-1137/38/9/090001.

[38] M. Arik et al., *Search for solar axions by the CERN axion solar telescope with $^3$he buffer gas: Closing the hot dark matter gap*, Physical Review Letters **112** (2014), no. 9, https://doi.org/10.1103%2Fphysrevlett.112.091302.

[39] R. Khatiwada et al., *Axion dark matter experiment: Detailed design and operations*, Review of Scientific Instruments **92** (2021), no. 12, 124502, https://doi.org/10.1063%2F5.0037857.

[40] H. Yoon, M. Ahn, B. Yang, Y. Lee, D. Kim, H. Park, B. Min, and J. Yoo, *Axion haloscope using an 18 t high temperature superconducting magnet*, Physical Review D **106** (2022), no. 9, https://doi.org/10.1103%2Fphysrevd.106.092007.

[41] M. Newville, T. Stensitzki, D. B. Allen, and A. Ingargiola, *Lmfit: Non-linear least-square minimization and curve-fitting for python*, Zenodo, September 2014, https://doi.org/10.5281/zenodo.11813.

[42] D. Baumann, *Tasi lectures on inflation*, 2009, https://arxiv.org/abs/0907.5424.

[43] K. Freese, *Natural inflation*, 1993.

[44] L. McAllister, E. Silverstein, and A. Westphal, *Gravity waves and linear inflation from axion monodromy*, Physical Review D **82** (2010), no. 4, https://doi.org/10.1103%2Fphysrevd.82.046003.

[45] E. Silverstein and A. Westphal, *Monodromy in the cmb: Gravity waves and string inflation*, Physical Review D **78** (2008), no. 10, https://doi.org/10.1103%2Fphysrevd.78.106003.

[46] J. Martin, C. Ringeval, R. Trotta, and V. Vennin, *The best inflationary models after planck*, Journal of Cosmology and Astroparticle Physics **2014** (2014), no. 03, 039–039, https://doi.org/10.1088%2F1475-7516%2F2014%2F03%2F039.

[47] J. Blanco-Pillado et al., *Racetrack inflation*, Journal of High Energy Physics **2004** (2004), no. 11, 063–063, https://doi.org/10.1088%2F1126-6708%2F2004%2F11%2F063.

[48] H. A. G. Ruiz, *Inflación con materia oscura dinámica*, 2022.